

Research Article

Tumor-Targeted Folic Acid-Modified Porfimer Conjugated Poly (Ethylene Glycol) Nanoparticles for Radiosensitized Treatment of Cancer

Song-Jin Pak[†], Chang-Jun Kim[†], Kwang-Il To^{†, *} , Nam-Hyok Ooh, Mun-Hyok Ri, Chol-Ho Ri, Nam-Yong Kim

Department of Nanomaterial, Institute of Chemistry and Biology, University of Sciences, Academy of Sciences, Pyongyang, DPR Korea

Abstract

Folic acid-modified porfimer conjugated poly (ethylene glycol) nanoparticles (FPP NPs), as the novel radiosensitizer, for tumor-targeted radiosensitized treatment (RST) were synthesized and characterized. Diamino poly (ethylene glycol) was covalently conjugated with folic acid and porfimer (also known as photofrin) in its terminal ends and self-assembled in aqueous solution to form FPP NPs. FPP NPs were characterized by FTIR spectrometer, zetasizer and transmission electron microscopy. FT-IR spectra of folic acid-modified porfimer conjugated poly (ethylene glycol) suggested that folic acid and porfimer were successfully covalently bound to poly (ethylene glycol) by amide bonds between carboxyl group and amino group. The average size and zeta potential of these nanoparticles were about 75nm and -13.5mV, respectively. And FPP NPs exhibited morphological features close to spherical shape by transmission electron microscopy observation. The loading efficiency and encapsulation efficiency of porfimer in FPP NPs were 8.52% and 45.67%, respectively. The experiments on reactive oxygen species (ROS) generation and cell viability showed that the nanoparticles could successfully suppress the growth of cancer cells by producing ROS with γ -ray irradiation. Furthermore, in vivo studies showed that FPP NPs exhibited the excellent tumor inhibition effect even at a half dose of free porfimer. These results suggested that FPP NPs would have potential for RST of the cancer.

Keywords

Porfimer, Folic Acid, Nanoparticles, Radiosensitizer

1. Introduction

Traditional cancer therapy, radiotherapy is the technique that induces tumor necrosis by irradiation of radiation such as X-ray and γ -ray, which produces the radicals and reactive oxygen species causing to excitation and ionization of bio-

molecules. RST is an advanced modality for cancer treatment, based on the cytotoxicity of active oxygen, which are produced by radiosensitizing reaction of tumor-selective radiosensitizer with the direct reaction of ionizing radiation. It is

*Corresponding author: tki1982@star-co.net.kp (Kwang-Il To)

[†] Song-Jin Pak, Chang-Jun Kim, Kwang-Il To are co-first authors.

Received: 7 April 2025; Accepted: 29 April 2025; Published: 12 June 2025



Copyright: © The Author(s), 2025. Published by Science Publishing Group. This is an **Open Access** article, distributed under the terms of the Creative Commons Attribution 4.0 License (<http://creativecommons.org/licenses/by/4.0/>), which permits unrestricted use, distribution and reproduction in any medium, provided the original work is properly cited.

confirmed that porphyrin photosensitizers being used for photodynamic therapy (PDT) have high sensitizing effect on ionizing radiation as well as visible light, therefore the radio-sensitized cancer treatment modality using the sensitizers is being introduced successfully in clinical. In particular, porfimer, a complex mixture of haematoporphyrin (Hp) oligomers, has been approved for PDT or RST of several tumors in clinical application [1].

Most photosensitizers, such as porfimer, are hydrophobic and may easily aggregate in a biological environment [2]. Moreover, the main problem of PDT or RST during and after clinical application is skin photosensitivity [3]. To overcome these limitations, nanocarriers for photosensitizers such as liposomes and polymeric micelles, have been studied [4, 5]. The nanocarriers with photosensitizers enhance the solubility. They also improve the tumor specificity of photosensitizers through enhanced permeability and retention (EPR) effect.

Surface modification of nanoparticles with the active targeting ligand enhances the selective accumulation into tumor cells. Such targeted drug delivery is a desirable strategy to improve the efficacy and safety of cancer treatment. Folic acid receptor (FR)- α is one of the most promising cell surface targets for the drug targeting. FR overexpresses on many cancer cell surfaces, including cancers of colon, lung, ovary, kidney and uterus [6-10].

Folic acid, which has a high affinity for the FR, enhances nanoparticle endocytosis through the FR. It is stable, inexpensive and poor immunogenic [11]. Conjugation of drugs and nanoparticles with folic acid can enhance their targeting ability and cell uptake via FR of cancer cell surface. Also, folic acid derivatives, which covalently conjugate with folic acid's γ -carboxyl moiety, can still possess a high affinity to the FR and maintain cell uptake ability via FR-mediated endocytosis comparably with folic acid. Several types of nanodrug carriers, including liposomes, polymeric nanoparticles, lipid nanoparticles, micelles and polymers, have been conjugated to folic acid for the targeted delivery [12].

In this paper, in order to enhance the selectivity to cancer cells and reduce the undesirable side-effect such as skin photosensitization by tumor-targeting the radiosensitizer, we synthesized the tumor-targeted radiosensitizer, FPP NPs and investigate the anti-cancer efficiency. Folic acid-modified porfimer conjugated poly (ethylene glycol) was synthesized by covalently conjugating terminal $-\text{NH}_2$ group of diamino poly (ethylene glycol) with $-\text{COOH}$ of folic acid and porfimer, followed by self-assembling into the nanoparticles in aqueous solution. Porfimer can be loaded into the nanoparticles at higher level by covalently conjugating to the carrier than it is spontaneously trapped in nanoparticles. Furthermore, the morphology, drug loading efficiency, in vitro RST and anti-cancer ability of this nanoparticle were investigated.

2. Material and Methods

2.1. Material

2.1.1. Chemicals

Porfimer (photofrin) was purchased from QLT (Vancouver, Canada) and 1, 3-diphenylisobenzofuran (DPBF) was purchased from Sigma Aldrich. Poly (ethylene glycol) (PEG, Mw: 4kDa) was obtained from Nektar (Huntsville, Alabama) and folic acid (FA) was obtained from TCI (Tokyo, Japan). N, N-dicyclohexylcarbodiimide (DCC), N-hydroxysuccinimide (NHS) and the other organic solvents were purchased from Aldrich Chemie (SteinheimWest-Germany).

2.1.2. Animals and Tumors

A549 cancer cell lines (human non-small cell lung cancer) was chosen as a tumor model. BALB/c mice, 6 weeks of age with a body weight of 20-22g, were used in experiments. The animals were subcutaneously injected in the outer region with 0.2ml of a sterile physiological solution containing about 1.5×10^6 A549 cells, and then estrogen was given by using an intragastric gavage to promote tumor growth. On the 7 day after transplantation, the tumors reached a volume of 80-100mm³, when the irradiation and pharmacokinetic experiments were adopted.

2.2. Methods

2.2.1. Synthesis of FPP NPs

(i). Synthesis of diamino poly (ethylene glycol)

Diamino poly (ethylene glycol) was synthesized and characterized as previously described [13]. In brief, 20g of poly (ethylene glycol) was placed in a 250ml dry triangular flask, vacuum-dried at 120 °C for 4h, followed by the addition of 100ml of anhydrous methylene chloride, 50ml pyridine, and 5g of paratoluenesulfonyl chloride and stayed in the dark at room temperature for 24h. The reaction solution was eluted and washed with 3mol/L HCl, and the organic layer was washed with 5g of NaHCO₃ and filtered to remove solvent to obtain poly (ethylene glycol)-paratoluenesulfonate crude. After dissolving in 8ml of tetrahydrofuran, the solution was slowly dropped into an excess of anhydrous ether to obtain a white precipitate and dried to obtain 18.6g of poly (ethylene glycol)-paratoluenesulfonate pure product.

Poly (ethylene glycol)-paratoluenesulfonate and 250mL of concentrated ammonia water were placed in a resisting pressure vessel and reacted at 140 °C for 6h. The reaction mixture was cooled to room temperature and extracted with equal volume of CH₂Cl₂ to obtain the diamino poly (ethylene glycol)-paratoluenesulfonate /CH₂Cl₂ solution.

An equal volume of 1mol/L of NaOH was thoroughly stirred for 2h, and the organic layer was washed with water to give the diamino poly (ethylene glycol) with amino groups at

its two ends.

(ii). *Synthesis of Folic acid-modified porfimer conjugated poly (ethylene glycol)*

Folic acid-modified porfimer conjugated poly (ethylene glycol) was synthesized by using the carbodiimide chemistry. In brief, triethylamine (200 μl), folic acid (300mg) and porfimer (1g) were dissolved in 10ml of dry DMSO under vigorous stirring. DCC (0.15g) and NHS (0.08g) were then added to the solution and the mixture was stirred for 8h in the dark at room temperature. After the side-product (dicyclohexyl urea, DCU) was removed by filtration, 10ml DMSO solution of $\text{NH}_2\text{-PEG-NH}_2$ (2g) was added by filtration and the reaction was carried out for 48 h at room temperature. Subsequently, the product was dialyzed with a dialysis tube (MWCO 6000) in DMSO for 3d to remove unreacted products and subsequently dialyzed with a dialysis tube (MWCO 1000) in deionized water for 3d to remove impurities and organic solvents. Finally, the Folic acid-modified porfimer conjugated poly (ethylene glycol) was freeze-dried and obtained as a red powder.

(iii). *Preparation of self-assembled FPP NPs*

FPP NPs were prepared via dialysis method. Folic acid-modified porfimer conjugated poly (ethylene glycol) can be self-organized in aqueous solution to form polymer nanoparticles due to the hydrophilic chain of poly (ethylene glycol) and the large hydrophobic ring of porfimer. Folic acid-modified porfimer conjugated poly (ethylene glycol) was dissolved in an appropriate amount of saline solution to form polymer nanoparticles. The whole process took place at room temperature.

2.2.2. Characterization of FPP NPs

The FTIR spectra of folic acid-modified porfimer conjugated poly (ethylene glycol) were recorded using a Nicolet 5700 FTIR spectrometer (Thermo Nicolet Corp., Denver, CO) under mild conditions. The average size and zeta-potential of the nanoparticles were determined by zetasizer (Malvern Zetasizer Nano ZS90, Malvern Instrument Co. Ltd., UK). The samples were placed in a cuvette and analyzed after ultrasonic dispersing for 30 min. The surface morphology of the nanoparticles was observed using a transmission electron microscope (JEOL 2010 UHR). The drug loading content (DL) and encapsulation efficiency (EE) of Porfimer were calculated according to the following equation:

$$\text{DL (\%)} = (\text{Weight of Porfimer in Nanodrug} / \text{Weight of Nanodrug}) \times 100\%$$

$$\text{EE (\%)} = (\text{Weight of Porfimer in Nanodrug} / \text{Weight of total Porfimer}) \times 100\%$$

2.2.3. Measurement of ROS

The chemical oxidation of 1, 3-diphenylisobenzofuran (DPBF) in aqueous solution of FPP NPs was used as an in-

direct method to measure singlet oxygen yield [14]. In this case, a decrease in the absorbance of DPBF added to the aqueous solution of FPP NPs was observed as a function of time after irradiating with γ -ray of 0.6Gy using ^{60}Co telera-diotherapy unit (AGAT-P1, 0.598Gy/min).

2.2.4. Cell Viability Assays and in Vitro RST

A549 cells were applied to investigate cell viability. 150 μL medium containing A549 breast tumor cells was added to 96-well plates at a density of $5 \times 10^4/\text{mL}$ and incubated at 37 $^\circ\text{C}$ for 24h under 5% CO_2 . Cells were exposed to suspensions of FPP NPs with different amounts of 1, 2, 4, 6, 8 and 10 $\mu\text{g}/\text{mL}$. After 24h, 20 μL 3-(4, 5-dimethylthiazole-2-yl)-2, 5-diphenyl-tetrazolium bromide (MTT) with a concentration of 5 $\mu\text{g}/\text{mL}$ was added to a 96-well plate and incubated at 37 $^\circ\text{C}$ for 4h. The culture supernatant was discarded and 150 μL DMSO was added to each well and stirred for 30min. The absorbance of the solution was measured using a microplate reader (Syneray-2, Biotek, USA) at 490 nm. To evaluate the radiotoxicity in vitro, ^{60}Co γ -rays were irradiated for 30min after 4h incubation for absorbing the nanoparticles and then incubated for 24h under the same conditions. A549 cells viability was expressed using the following formula:

$$\text{Viability (\%)} = ((\text{OD}_{\text{sample}} - \text{OD}_{\text{zero}}) / (\text{OD}_{\text{control}} - \text{OD}_{\text{zero}})) \times 100\%$$

The value of $\text{OD}_{\text{sample}}$ was provided by drug-treated cells, $\text{OD}_{\text{control}}$ values were provided by drug-free cells, and OD_{zero} values were obtained from both drug- and cell-free wells [15].

2.2.5. In Vivo Efficacy

Mice were used to investigate the anticancer ability of FPP NPs in vivo. A549 cells (1.5×10^6 cells/0.1mL) were injected into the oter of mice, and then estrogen was given by intra-gastric gavage to promote tumor growth. Mice were randomly divided into four groups when the tumor volume reached 80-100 mm^3 , which were denoted as control (normal saline without irradiation), normal saline + irradiation, free porfimer (20mg/kg) + irradiation and FPP NPs (10mg/kg of free porfimer equivalents) + irradiation. All groups (excepting control group) were irradiated with ^{60}Co γ -rays within 30 min after 24 h of injection. Therapeutic effects were assessed by measuring tumor volume in the 4 groups treated every 3 days. Body weight was measured to assess drug safety in four treated groups every 3 days [16]. Tumor volume was calculated by applying the expression $V = 4\pi/3 \times l/2 \times w/2 \times h$. Herein, l is the longer diameter, w is the shorter diameter, and h is the height of the hemielliptic tumor. The inhibition rate was calculated by the following equation:

$$\text{Inhibition rate (\%)} = (V_c - V_e) / V_c \times 100\%,$$

where in V_c is the average tumor volume of control group and V_e is the average tumor volume of experimental group [17].

Each assay was performed in triplicate ($n=3$). Results were expressed as the mean \pm standard deviation (SD). Analysis of variance (ANOVA) was used to evaluate the comparison of formulations.

3. Results and Discussion

3.1. Preparation and Characterization of FPP NPs

The scheme of the synthesis of FPP NPs and the passive and active targeted drug delivery was shown in Figure 1.

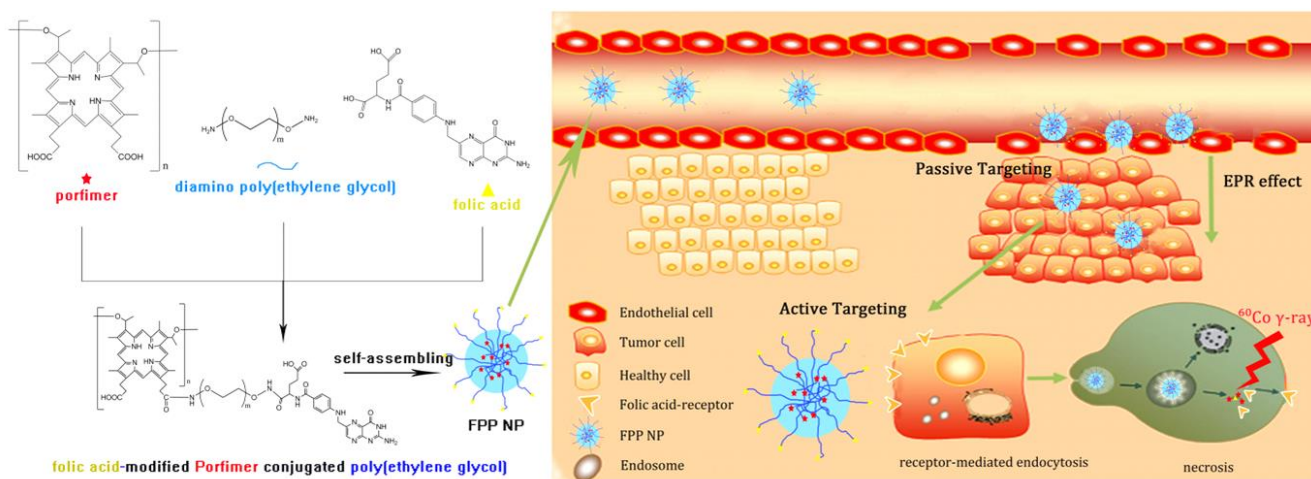


Figure 1. Schematic illustration of preparation and tumor-targeting of FPP NPs for RST of cancer.

Diamino poly (ethylene glycol) as a nanocarrier was synthesized based on the literature and the amino substitution of diamino poly (ethylene glycol) was measured by titration and calculated as 87.8% according to the formula [13].

Folic acid-modified porfimer conjugated poly (ethylene glycol) was synthesized via covalently conjugating the two-terminal amino groups of diamino poly (ethylene glycol) with the carboxyl groups of folic acid and porfimer using carbodiimide chemistry.

The FT-IR spectra of pure folic acid, porfimer, poly (ethylene glycol), diamino poly (ethylene glycol), folic acid-modified poly (ethylene glycol) and folic acid-modified porfimer conjugated poly (ethylene glycol) were shown in Figure 2. In the pure poly (ethylene glycol), diamino poly (ethylene glycol), folic acid-modified poly (ethylene glycol) and folic acid-modified porfimer conjugated poly (ethylene glycol), the absorption bands at 2883 and 1467 cm^{-1} were assigned to the stretching vibration and bending vibration of C-H, respectively and the peak at about 1100 cm^{-1} was assigned to the asymmetric stretching vibrations of C-O-C. The

absorption bands at 1635 cm^{-1} were assigned to the stretching vibration of C-N and bending vibration of N-H in diamino poly (ethylene glycol), confirming the successful synthesis of $\text{NH}_2\text{-PEG-NH}_2$. This absorption band also is known as the amide I band. The amide I band represents 80% of the C=O stretching vibration of the amide group coupled to the in-plane N-H bending and C-N stretching modes. In diamino poly (ethylene glycol), folic acid-modified poly (ethylene glycol) and Folic acid-modified porfimer conjugated poly (ethylene glycol), the absorbances in this region were different each other, the rate of the absorbance in 1635 cm^{-1} to 1114 cm^{-1} can represent the degree of conjugating $-\text{NH}_2$ of diamino poly (ethylene glycol) with $-\text{COOH}$ of folic acid-modified poly (ethylene glycol) and folic acid-modified porfimer conjugated poly (ethylene glycol). These rates in folic acid-modified poly (ethylene glycol) and folic acid-modified porfimer conjugated poly (ethylene glycol) were 1.3 and 1.7 times higher than that of diamino poly (ethylene glycol), suggesting that folic acid and porfimer were successfully covalently bound to poly (ethylene glycol).

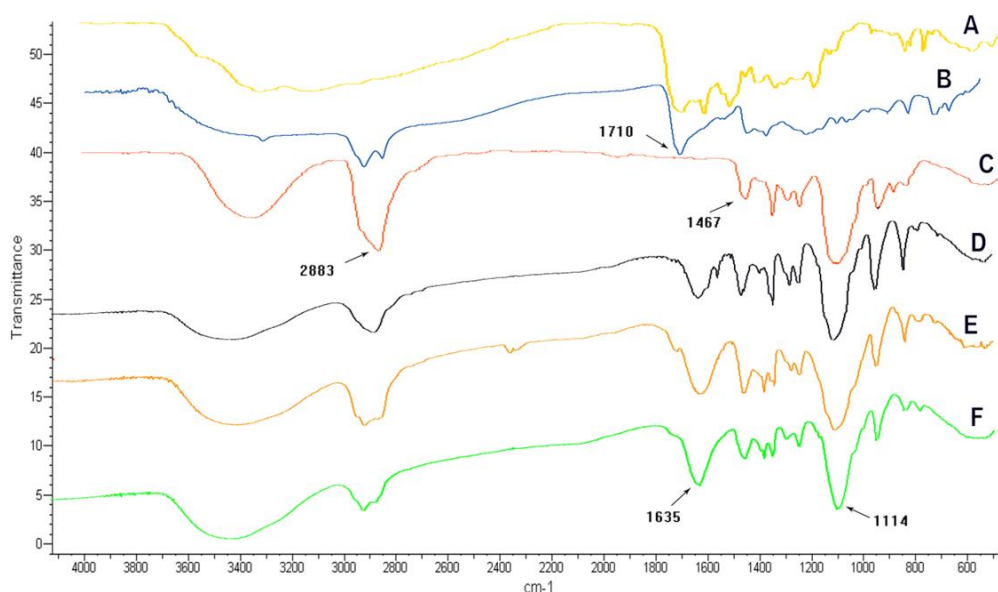


Figure 2. FT-IR spectra of folic acid (A), porfimer (B), poly (ethylene glycol)(C), diamino poly (ethylene glycol)(D), folic acid-modified poly (ethylene glycol)(E) and folic acid-modified porfimer conjugated poly (ethylene glycol)(F).

Folic acid-modified porfimer conjugated poly (ethylene glycol) was self-assembled in aqueous solution during dialysis to form nanoparticles (Figure 1). The average size, zeta potential and TEM micrographs of the FPP NPs are shown in Figure 3. The average size and zeta potential of these nanoparticles were about 75nm and -13.5mV, respectively. As shown in Figure 3c, TEM image revealed that these nanoparticles exhibited morphological features close to spherical

shape.

The drug loading content and encapsulation efficiency of the porfimer were calculated according to the formula [15] and were about 8.52% and 45.67%, respectively. The porfimer drug loading content of these nanoparticles, which was synthesized by covalently conjugating the drug to the nanocarrier, seems to be higher compared to the non-covalent trapping way.

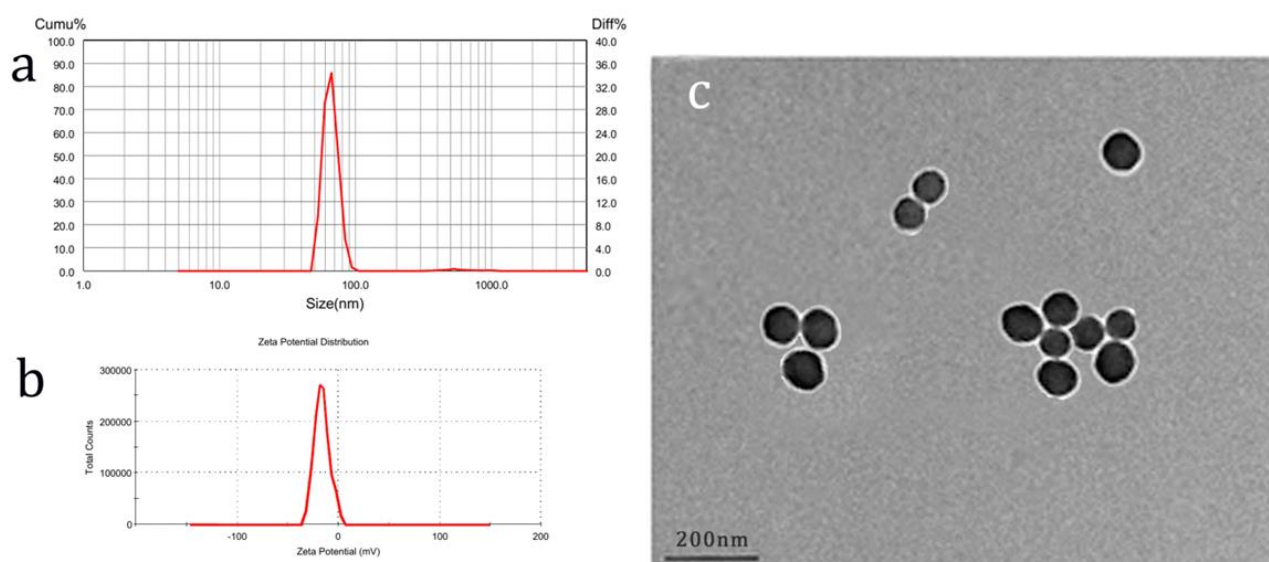


Figure 3. (A, B) The size distribution and zeta potential of FPP NPs,(C) The TEM image of FPP NPs.

3.2. ROS Detection

The emitted $^1\text{O}_2$ was indirectly detected using DPBF as $^1\text{O}_2$ chemical probe [14]. DPBF reacted irreversibly with $^1\text{O}_2$ excited from the porfimer by radiation, and the reaction was confirmed by measuring the extinction intensity of DPBF at 407 nm. Figure 4A showed the change in the absorption spectrum of DPBF with time after irradiation for free porfimer and FPP NPs. As shown in the figure, both free porfimer and FPP NPs showed a significant decrease in absorbance compared to the control, indicating that the free porfimer and the FPP NPs produced $^1\text{O}_2$ efficiently by radiation. The generation efficiency of $^1\text{O}_2$ was not significantly different between free porfimer and nanodrug. This result confirmed that the nanoparticles have no inhibitory effect on the generation of the ROS by radiosensitizer.

3.3. Cell Viability Assays and in Vitro RST

Cell viability assays and in vitro RST were performed on

human non-small cell lung cancer A549 cancer cells using MTT assay. As shown in Figure 4B, free porfimer and FPP NPs showed no significant difference in cell viability in the dark, and both showed high viability even with increased concentrations. These results indicated that the toxicity to the normal cells did not increase significantly with increasing concentrations of free porfimer or nanodrug. As shown in Figure 4C, the cytotoxicity showed a significant increase with increasing drug concentration in the presence of radiation. It was also shown that the cytotoxicity of FPP NPs was clearly higher than that of free porfimer. Therefore, we concluded that FPP NPs have the ability to more efficiently kill cancer cells under irradiation. This effect of FPP NPs may be attributed to more accumulation of the radiosensitizers in cancer cells due to passive targeting via EPR effect and active targeting via folic acid receptor-mediated endocytosis to cancer cells [12]. (Figure 1).

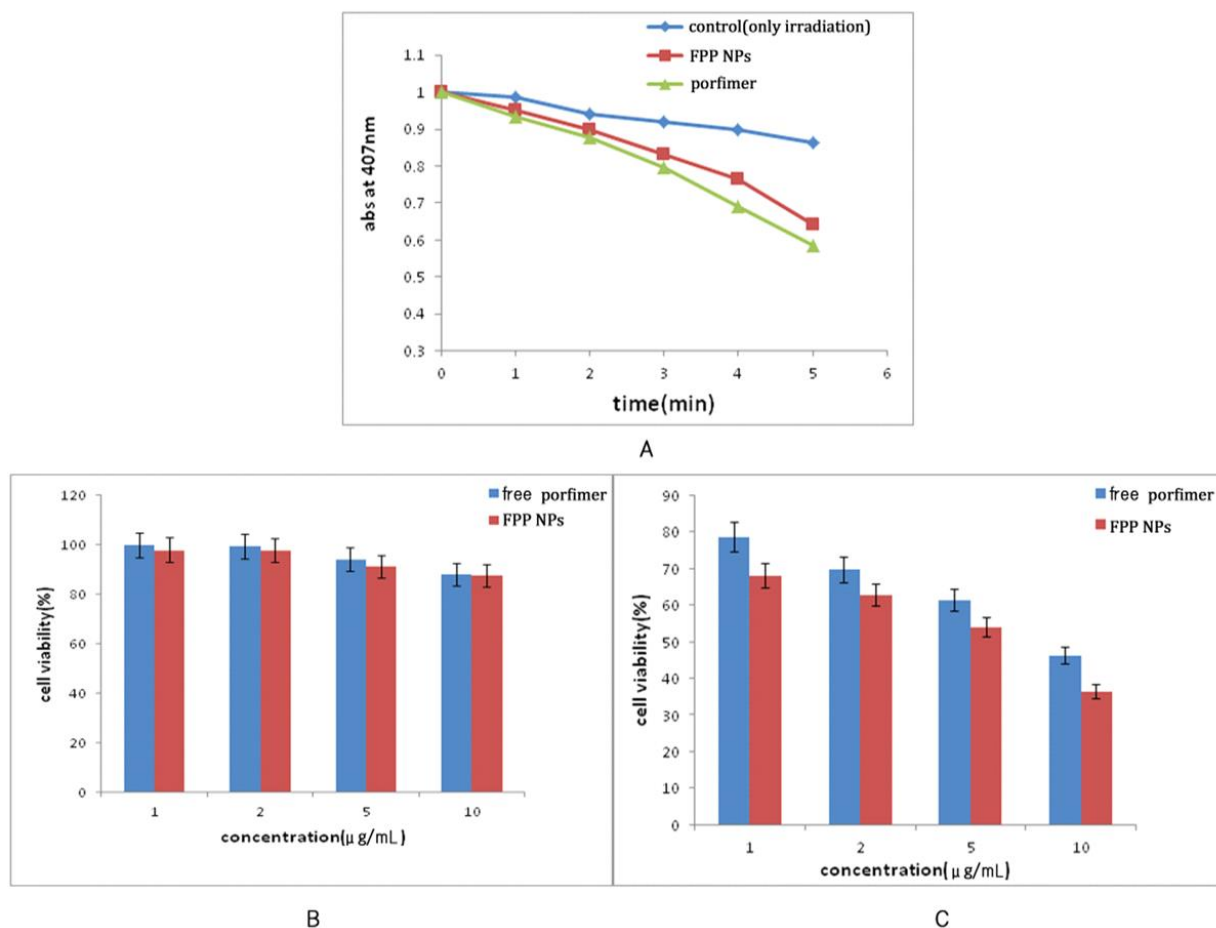


Figure 4. Absorbance at 407nm measured every minute of irradiation with ^{60}Co γ -ray for DPBF in the presence of porfimer or FPP NPs and free DPBF (A) and A549 cells viability of free porfimer and FPP NPs without (B) or with (C) irradiation. The results represent the mean \pm standard deviation ($n = 3$).

3.4. In Vivo Effect

As shown in Figure 5A, control showed continuous tumor growth, whereas free porfimer-treated and FPP NPs-treated groups showed significant inhibitory effects on tumor growth compared to control. The irradiated group showed a slight inhibitory effect compared to the control group. The FPP NPs group showed similar tumor inhibition, although only half dose of the drug was applied compared to free porfimer-treated group (Figure 5C). This is evidence that FPP NPs accumulated in high concentrations in tumor tissue

compared to free porfimer to enhance radiosensitizing activity, thus inhibiting tumor growth. On the other hand, relative body weight was measured to evaluate the stability of FPP NPs. As shown in Figure 5B, there was no significant weight loss and no significant difference in all groups, indicating good biostability of the nanodrug.

These data supported our hypothesis that FPP NPs can selectively accumulate in tumor cells and efficiently generate ROS under irradiation, thereby enhancing the radiosensitive effect of the porfimer and reducing the side-effects, such as skin photosensitivity, by reducing its dose for RST of cancers.

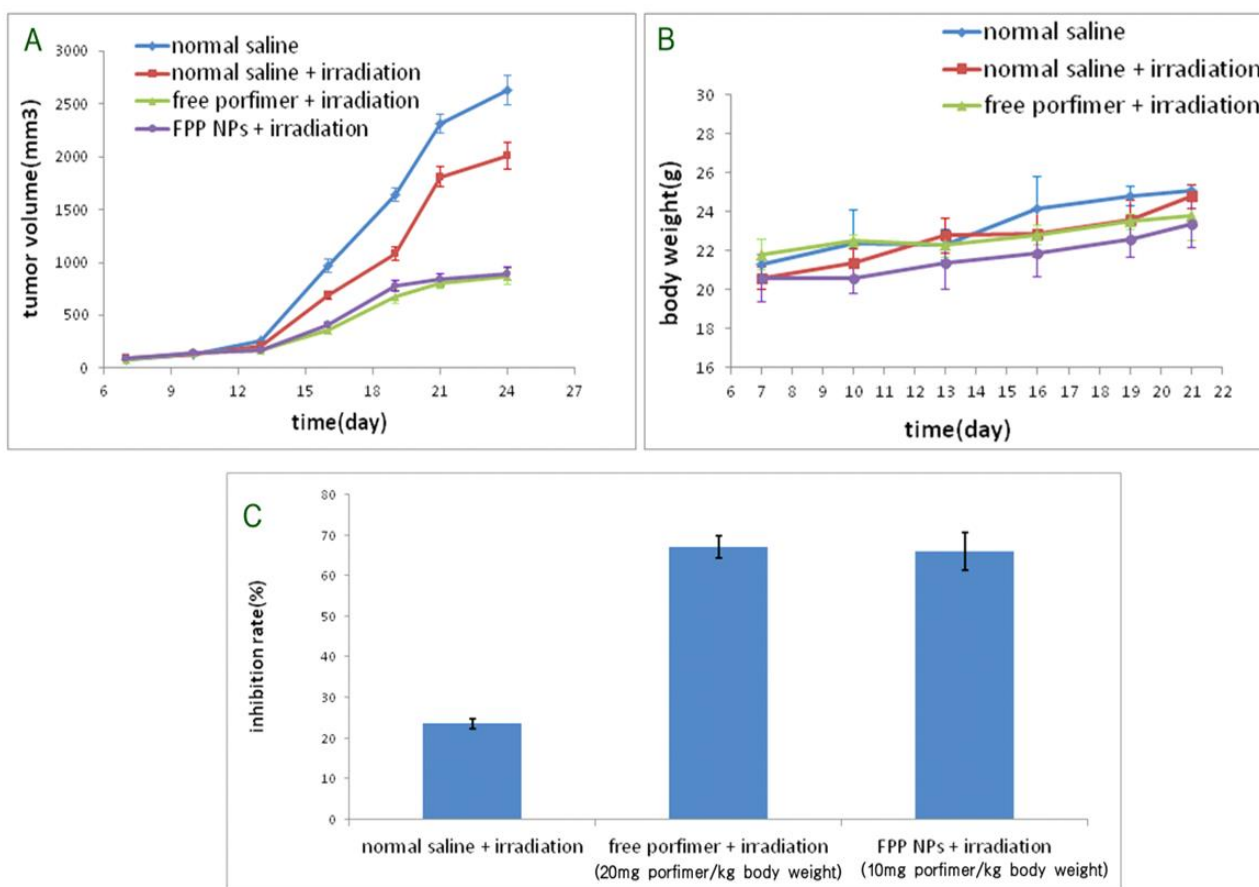


Figure 5. In vivo antitumor efficacy evaluation of free porfimer and FPP NPs with ⁶⁰Co γ -ray irradiation (A) tumor volume changes over treatment times, (B) the body weight changes of tumor-bearing mice, (C) inhibition rate. The results represent the mean \pm standard deviation ($n = 3$).

In this paper, we described the novel FPP NPs for RST of cancer. Folic acid-modified porfimer conjugated poly (ethylene glycol) was self-assembled in aqueous suspension into the nanoparticles, which were given the proper nano-scaled size, high dispersity and stability. The study on ROS generation showed that these nanoparticles had the ability to produce ROS in response to ⁶⁰Co γ -ray comparably with free porfimer. In vitro cytotoxicity of these nanoparticles showed rather higher killing effect against A549 cancer cell lines than free porfimer. This result suggested that FPP NPs would effectively accumulate in cancer cell through folic acid recep-

tor-mediated endocytosis. In vivo experiment confirmed that FPP Nps could exhibit the similar anti-cancer effect to free porfimer even at a half dose of free porfimer, which proved that FPP NPs could be the potential candidate for RST of cancer.

4. Conclusion

In this paper, we described the novel FPP NPs for RST of cancer. Folic acid-modified porfimer conjugated poly

(ethylene glycol) was self-assembled in aqueous suspension into the nanoparticles, which were given the proper nano-scaled size, high dispersity and stability. The study on ROS generation showed that these nanoparticles had the ability to produce ROS in response to ^{60}Co γ -ray comparably with free porfimer. In vitro cytotoxicity of these nanoparticles showed rather higher killing effect against A549 cancer cell lines than free porfimer. This result suggested that FPP NPs would effectively accumulate in cancer cell through folic acid receptor-mediated endocytosis. In vivo experiment confirmed that FPP NPs could exhibit the similar anti-cancer effect to free porfimer even at a half dose of free porfimer, which proved that FPP NPs could be the potential candidate for RST of cancer.

Abbreviations

FPP NPs	Folic Acid-modified Porfimer Conjugated Poly (Ethylene Glycol) Nanoparticles
RST	Radiosensitized Treatment
ROS	Reactive Oxygen Species
PDT	Photodynamic Therapy
EPR	Enhanced Permeability and Retention
FR	Folic Acid Receptor
DCC	N, N-dicyclohexylcarbodiimide
NHS	N-hydroxysuccinimide
DCU	Dicyclohexyl Urea
DPBF	1, 3-diphenylisobenzofuran
PEG	Poly (Ethylene Glycol)

Author Contributions

Song-Jin Pak: designed manuscript

Chang-Jun Kim: performed experiment

Kwang-II To: corrected and finalized manuscript

Nam-Hyok O: conceptualized and performed experiment

Mun-Hyok Ri: analyzed data, revised draft and supervised

Chol-Ho Ri: analyzed data, revised draft and supervised

Nam-Yong Kim: conceptualized and performed experiment

Ethical Statement

All animal experiments were performed in accordance with the regulations of the Administration of Affairs Concerning Experimental Animals in DPR Korea. The study protocol was approved by the Institutional Animal Care and Use Committee of the Pyongyang University Science and Technology.

Conflicts of Interest

The authors declare no conflicts of interest.

References

- [1] M. Vogeser et al., Development of an HPLC method for monitoring of Photofrin II therapy, *Clinical Biochemistry*, 38, 73–78(2005). <https://doi.org/10.1016/j.clinbiochem.2004.09.014>
- [2] Ł. Lamch, et al., Folate-directed zinc (II) phthalocyanine loaded polymeric micelles engineered to generate reactive oxygen species for efficacious photodynamic therapy of cancer, *Photodiagnosis and Photodynamic Therapy*, 25 480–491(2019). <https://doi.org/10.1016/j.pdpdt.2019.02.014>
- [3] I. J. MACDONALD AND T. J. DOUGHERTY, Basic principles of photodynamic therapy, *J. Porphyrins Phthalocyanines*, 5, 105–129(2001).
- [4] Hailong Qiu, Meiling Tan, Tymish Y. Ohulchanskyy, Jonathan F. Lovell and Guanying Chen, Recent Progress in Upconversion Photodynamic Therapy, *Nanomaterials*, 8(344), 1-18(2018). <https://doi.org/10.3390/nano8050344>
- [5] Cornelus F. van Nostrum, Polymeric micelles to deliver photosensitizers for photodynamic therapy. *Adv. Drug Delivery Rev.*, 56, 9–16(2004). <https://doi.org/10.1016/j.addr.2003.07.013>
- [6] E. A. Henderson et al., Targeting the α -folate receptor with cyclopenta [g] quinazoline-based inhibitors of thymidylate synthase, *Bioorg. Med. Chem.*, 14, 5020–5042(2006). <https://doi.org/10.1016/j.bmc.2006.03.001>
- [7] S Mohapatra et al., Synthesis of highly stable folic acid conjugated magnetite nanoparticles for targeting cancer cells, *Nanotechnology*, 18, 1-9(2007). <https://doi.org/10.1088/0957-4484/18/38/385102>
- [8] S. Mansouri et al., Characterization of folate-chitosan-DNA nanoparticles for gene therapy, *Biomaterials*, 27, 2060–2065(2006). <https://doi.org/10.1016/j.biomaterials.2005.09.020>
- [9] M. O. Oyewumi et al., Comparison of cell uptake, biodistribution and tumor retention of folate-coated and PEG-coated gadolinium nanoparticles in tumor-bearing mice, *Journal of Controlled Release*, 95, 613–626(2004). <https://doi.org/10.1016/j.jconrel.2004.01.002>
- [10] Liu S. Q. et al., Bio-functional micelles self-assembled from a folate-conjugated block copolymer for targeted intracellular delivery of anticancer drugs. *Biomaterials*, 28, 1423–1433(2007). <https://doi.org/10.1016/j.biomaterials.2006.11.013>
- [11] C. Huang et al., Magnetic micelles as a potential platform for dual targeted drug delivery in cancer therapy, *International Journal of Pharmaceutics*, 429, 113–122(2012). <https://doi.org/10.1016/j.ijpharm.2012.03.001>
- [12] Zhao X. et al. Targeted drug delivery via folate receptors, *Expert Opin. Drug Deliv.*, 5(3), 309-319(2008). <http://dx.doi.org/10.1517/17425247.5.3.309>
- [13] S. Zhang et al., Synthesis of heterobifunctional poly (ethylene glycol) with a primary amino group at one end and a carboxylate group at the other end, *Reactive & Functional Polymers*, 56, 17–25(2003). [https://doi.org/10.1016/S1381-5148\(03\)00015-4](https://doi.org/10.1016/S1381-5148(03)00015-4)

- [14] Qian J. et al., Colloidal mesoporous silica nanoparticles with protoporphyrin IX encapsulated for photodynamic therapy. *J. Biomed. Opt.*, 14(1), 014012(2009).
<https://doi.org/10.1117/1.3083427>
- [15] Yu Y. et al., Protoporphyrin IX-loaded laminarin nanoparticles for anticancer treatment, their cellular behavior, ROS detection, and animal studies, *Nanoscale Res. Lett.*, 14(316), 1-12(2019).
<https://doi.org/10.1186/s11671-019-3138-0>
- [16] Wang K. L. et al., In vivo evaluation of reduction-responsive alendronate-hyaluronan-curcumin polymer-drug conjugates for targeted Therapy of bone metastatic breast cancer, *Molecular Pharm.*, 15(7), 2764–2769(2018).
<https://doi.org/10.1021/acs.molpharmaceut.8b00266>
- [17] Luksiene Z. et al., Radiosensitization of tumours by porphyrins, *Cancer Letters*, 235, 40–47(2006).
<https://doi.org/10.1016/j.canlet.2005.03.041>